

1 **Machine Learning-GWAS reveals the role of *WSD1* gene for cuticular wax ester  
2 biosynthesis and key genomic regions controlling early maturity in bread wheat.**

3

4 Honoré Tekeu<sup>1,2,3</sup>, Martine Jean<sup>1,2</sup>, Eddy L. M. Ngonkeu<sup>3</sup>, François Belzile<sup>1,2\*</sup>

5 Corresponding author: [francois.belzile@fsaa.ulaval.ca](mailto:francois.belzile@fsaa.ulaval.ca)

6 <sup>1</sup>Département de Phytologie, Université Laval, Quebec City, QC, Canada

7 <sup>2</sup>Institut de Biologie Intégrative et des Systèmes (IBIS), Université Laval, Quebec City, QC,  
8 Canada

9 <sup>3</sup>Institute of Agricultural Research for Development, Yaoundé, Cameroon.

10

11 **Abstract**

12

13 This study employed Machine Learning-Genome-Wide Association Study (ML-GWAS) to  
14 identify genomic regions linked to cuticular wax ester biosynthesis (SW) and early maturity  
15 (DM) in wheat. Using a dataset with 170 wheat accessions and 74K SNPs, four GWAS tools  
16 (MLM, CMLM, FarmCPU, and BLINK) and five machine learning techniques (RF, ANN,  
17 SVR, CNN, and SVM) were applied. A highly significant SW association was found on  
18 chromosome 1A, with the peak SNP (chr1A:556842331) explaining 50% of the phenotypic  
19 variation. A promising candidate gene, *TraesCS1A01G385500*, was identified as an ortholog  
20 of *Arabidopsis thaliana*'s *WSD1* gene, which plays a crucial role in very long-chain (VLC) wax  
21 ester biosynthesis. For DM, four QTLs were detected on chromosomes 4B (two QTLs), 2A,  
22 and 5A. Haplotype analysis revealed that alleles TT significantly contribute to cuticular wax  
23 ester biosynthesis and early maturity in wheat varieties. The study underscores the superior  
24 performance of ML models, especially when combined with advanced multi-locus GWAS  
25 models like BLINK and FarmCPU, with significantly lower p-values for identifying relevant  
26 QTLs compared to traditional methods. ML approaches hold potential for revolutionizing the  
27 study of complex genetic traits, offering insights to enhance wheat crops' resilience and quality.  
28 ML-GWAS emerges as a compelling tool for genomic-based breeding, enabling breeders to  
29 develop improved wheat varieties with greater precision and efficiency.

30

31 **Keywords:** International wheat collection, Genotyping-by-Sequencing, population structure,  
32 Genome-Wide Association Study, Machine learning, spike waxiness, number of days-to-  
33 maturity.

34

35

36

37

38

39

40

41

42

43

44

45

46 **Introduction**

47

48 Wheat (*Triticum aestivum* L.), a globally essential staple crop, faces a multitude of  
49 environmental challenges, from drought and salinity to extreme temperatures and pest pressures  
50 (He et al., 2022). A vital component of its adaptive response to these challenges is the  
51 hydrophobic cuticle, composed of cutin and cuticular waxes (Wang and Chang, 2022). This  
52 lipidic shield defends against non-stomatal transpiration, UV radiation, pathogens, and insect  
53 invasions while maintaining the integrity of adjacent plant organs (Ingram and Nawrath, 2017;  
54 Martin and Rose, 2014).

55 The cuticle consists of two primary constituents: cutin, an insoluble polyester, and cuticular  
56 waxes, encompassing very-long-chain (VLC) fatty acids, aldehydes, ketones, esters, alcohols,  
57 alkanes, and other compounds (Kunst and Samuels, 2009). Alkanes, a significant component  
58 of cuticular waxes, play a critical role in enhancing plant drought tolerance (Kosma et al., 2009;  
59 Seo et al., 2011). In the realm of wheat, genes related to wax biosynthesis, including TaFARs  
60 for primary alcohols and the W1 locus for  $\beta$ -diketones, have been identified (Hen-Avivi et al.,  
61 2016; Y. Wang et al., 2015a, 2015b). One pivotal gene, TaCER1-1A, has been recognized for  
62 its involvement in alkane accumulation in wheat (Li et al., 2019). In a recent study by (He et  
63 al., 2022), attention is drawn to TaCER1-6A, another key gene involved in alkane biosynthesis  
64 in wheat, with investigations extending to overexpression and CRISPR/Cas9-mediated gene  
65 editing.

66 To date, no study has pinpointed a gene responsible for the biosynthesis of wax VLC esters,  
67 which play a crucial role in mitigating leaf water loss, particularly under drought conditions.  
68 The journey of these wax constituents from the Golgi and trans-Golgi network (TGN) to the  
69 plasma membrane and onward to the cuticle involves pathways coordinated by ABCG  
70 subfamily half transporters and lipid transfer proteins (LTPs) (DeBono et al., 2009; Ichino and  
71 Yazaki, 2022; Pighin et al., 2004; Wang and Chang, 2022).

72

73 Additionally, the cultivation of early-maturing wheat varieties holds critical importance in  
74 regions characterized by short growing seasons and extended daylight, exemplified by the  
75 Northern Great Plains of Canada and the USA (A. Kamran et al., 2013). Early maturation not  
76 only enhances crop yields but also acts as a safeguard against frost damage, a threat that can  
77 significantly compromise grain quality and overall agricultural productivity (Iqbal et al., 2007).  
78 The precise timing of wheat's flowering is intricately regulated by a complex interplay of genes  
79 that dictate growth patterns and earliness. These genetic regulators encompass vernalization

80 (Vrn), photoperiod (Ppd), and earliness per se (Eps) genes, shaping when wheat plants initiate  
81 flowering and influencing their growth habits (Atif Kamran et al., 2013).

82 Adding to this complexity, certain genetic factors, such as dwarfing genes, subtly affect the  
83 timing of heading, flowering, and maturity, introducing further intricacies in the regulation of  
84 these vital agricultural traits (Chen et al., 2018; Daoura Goudia et al., 2014). Earliness per se  
85 genes also play a role in enhancing the adaptability of wheat plants, contributing to their  
86 resilience in varying environments (Snape et al., 2001). Recent studies, including one by  
87 Semagn et al. (2021), have delved into the intricate genetic mapping of Quantitative Trait Loci  
88 (QTLs) associated with days to maturity, particularly in wheat varieties evaluated under both  
89 conventional and organic farming practices. These studies have identified key QTLs on  
90 chromosome 4B, shedding light on the genetic mechanisms governing maturity. Furthermore,  
91 earlier research by authors such as (Zou et al., 2017a, 2017b) employing extensive genetic  
92 mapping using 1203 markers in RIL populations like 'Attila' and 'CDC Go' has uncovered a  
93 shared genomic region linked to maturity, situated on both chromosome 4B and 5A.

94 Among the array of genetic factors at play, certain dwarfing genes, including Rht-B1, Rht5,  
95 Rht8, and Rht12, have been identified as contributing factors, subtly influencing the timing of  
96 heading, flowering, and maturity in wheat varieties. These genetic elements add an additional  
97 layer of complexity to the intricate regulation of these pivotal traits (Chen et al., 2018; Daoura  
98 Goudia et al., 2014).

99

100 While molecular markers have facilitated characterizing genetic diversity, phenotypic  
101 assessments have primarily determined the utility of these genetic resources in breeding (Belzile  
102 et al., 2020). With the availability of high-density SNP markers, Genome-Wide Association  
103 Studies (GWAS) have become a powerful tool for identifying and mapping loci contributing to  
104 phenotypic variation among diverse genetic materials that have undergone extensive  
105 recombination (Yu and Buckler, 2006). Recent applications of highly reproducible GBS-  
106 derived SNPs have uncovered candidate genes influencing grain size in bread wheat (Tekeu et  
107 al., 2021). GWAS has become a standard approach across species for identifying genes  
108 associated with critical traits (Ashkenazy et al., 2022).

109 However, there remain challenges with conventional GWAS techniques, including the "large  
110 p, small n" issue when the number of markers surpasses the number of genotypes (Kaler et al.,  
111 2020; Mohammadi et al., 2020). Conventional GWAS methods are better suited for identifying  
112 common SNPs with substantial main effects, while the distinction between causal variants and

113 correlated genes linked by linkage disequilibrium remains problematic (Enoma et al., 2022;  
114 Nicholls et al., 2020). Moreover, conventional GWAS approaches lack the power to uncover  
115 minor-effect SNPs associated with specific traits (Zhou et al., 2019). Consequently, machine  
116 learning (ML) techniques offer an opportunity to address these limitations and gain insights  
117 into the complex genetic basis of traits, as demonstrated in other crop species (Ashkenazy et  
118 al., 2022; Kwon et al., 2022).

119 Machine learning models for GWAS vary in complexity, from simple logistic regression to  
120 sophisticated ensemble models such as random forests, gradient boosting, and neural networks.  
121 These ML algorithms focus on maximizing prediction accuracy and excel at capturing multi-  
122 locus SNP interactions better than conventional methods. Support Vector Regression (SVR) is  
123 one such machine learning technique that has shown promise in predicting important  
124 agricultural traits (Yoosefzadeh Najafabadi et al., 2021). While SVR has found application in  
125 various crop studies, the potential of other ML techniques, such as Random Forest (RF),  
126 Convolutional Neural Networks (CNN), Artificial Neural Networks (ANN), and Support  
127 Vector Machines (SVM), remains largely untapped when compared to the more conventional  
128 GWAS tools like Mixed Linear Model (MLM), Compressed Mixed Linear Model (CMLM),  
129 Fixed and random model Circulating Probability Unification (FarmCPU), and Bayesian-  
130 information and Linkage-disequilibrium Iteratively Nested Keyway (BLINK).

131 This study aims to address this gap and provide valuable insights to bolster crop resilience. By  
132 employing a diverse array of advanced ML techniques in GWAS analysis, we seek to identify  
133 the genomic regions associated with cuticular wax ester biosynthesis (SW) and early maturity  
134 (DM) in wheat. Our approach promises to shed light on the intricate genetic mechanisms  
135 governing these vital traits and contribute to the advancement of crop breeding efforts for  
136 improved wheat varieties. Our research hypotheses revolve around specific genomic regions  
137 influencing SW and DM in a diverse global collection of bread wheat accessions. Furthermore,  
138 it postulates that ML-GWAS approaches will outperform traditional GWAS methods, in  
139 identifying Quantitative Trait Loci (QTLs) relevant to SW and DM traits in wheat. The present  
140 study aims to decipher the genetic underpinnings of SW and DM using ML-GWAS approaches.

141 **Materials and methods**

142 **Plant materials**

143 In this study, an international collection of 170 accessions was employed for genome-wide  
144 association analyses. These cultivars were obtained from various international wheat breeding  
145 programs. The South African accessions consisted of spring wheat lines from the Western Cape  
146 region, along with some winter bread wheat lines from other parts of the country. The East  
147 African spring-type accessions were gathered in Kenya and Ethiopia. The Mexican accessions  
148 were obtained via the International Maize and Wheat Improvement Center (CIMMYT), and  
149 they included spring accessions from Mexicali and Baja California. The Central African  
150 accessions were provided by the Institute of Agricultural Research for Development (IRAD)  
151 and farmers (Tekeu et al., 2017). The French accessions were winter lines, and those from North  
152 Africa were composed of spring lines acquired from the International Center for Agricultural  
153 Research in the Dry Areas (ICARDA).

154 **Phenotyping**

155 A panel of 170 accessions of bread wheat was phenotyped and used for genome-wide  
156 association analyses. Field trials were conducted in two different locations in the bimodal humid  
157 forest zone of Cameroon, during the 2015-2016 season in Munt Mbankolo (1057 m above sea  
158 level) and during 2016-2017 in Nkolbisson (650 m a. s. l.). At each trial site, an incomplete  
159 alpha-lattice design with two replications was used and each accession was planted, as  
160 previously reported by (Tekeu et al., 2021). Then, fields trials were managed in accordance  
161 with the technical recommendations and standard agricultural practices for wheat (Pask et al.,  
162 2012). Spike waxiness (SW; 0: Absent, 2: Almost none, 3: Very little, 4: Little, 5: Intermediate,  
163 6: Some, 7: Much, 8: Very much) and DM (days-to-maturity) were assessed when 50% of  
164 spikes had turned yellow (Zadoks et al., 1974).

165

166 **Analysis of phenotypic data**

167 We conducted the analysis of variance for each trait using PROC MIXED in SAS 9.4. In this  
168 analysis, each cultivar was considered a fixed effect, while replications and environments were  
169 treated as random effects. Pearson correlation coefficients between pairs of phenotypic traits  
170 were computed using Pearson's correlation in SPSS 20.0. To assess the heritability of each trait,  
171 we utilized the broad-sense heritability ( $h^2$ ) formula:  $h^2 = VG / (VG + VGE + Ve)$ , where VG

172 represents genetic variance, VGE is the genetic-environment interaction variance, and Ve is the  
173 error variance.

174 **DNA isolation, GBS library construction and sequencing**

175 To extract genomic DNA from dried young leaf tissue (~ 5 mg) of all accessions, we used a  
176 CTAB DNA isolation method (Doyle and Doyle, 1990). The extracted DNA was quantified  
177 using a Quant-iT™ PicoGreen kit (ThermoFisher Scientific, Canada), and concentrations were  
178 normalized to 20 ng/µl for library preparation. We constructed three 96-plex *PstI-MspI* GBS  
179 libraries as described by (Elshire et al., 2011). Subsequently, each library was sequenced on  
180 three P1 chips using an Ion Torrent PGM sequencer at the Plate-forme d'Analyses Génomiques  
181 of the Institut de Biologie Intégrative et des Systèmes (Université Laval, Québec, Canada).

182 **Single nucleotide polymorphism calling and bioinformatics analysis.**

183 Genomic DNA sequences of wheat samples, with an average of 2.4 million reads per wheat  
184 line, were analyzed using the FastGBS pipeline (Torkamaneh et al., 2017). The reads were  
185 aligned to the wheat reference genome (Chinese Spring v1.0), and SNPs were called using  
186 FastGBS. Standard filtration steps were applied to the FastGBS results, as previously described  
187 by (Tekeu et al., 2021). Additional filtration steps were carried out on this subset to retain only  
188 SNPs with a minor allele frequency (MAF) of at least 0.05.

189  
190 **Machine Learning-Genome-Wide Association Study**

191  
192 We conducted a genome-wide association study (GWAS) to identify genomic regions  
193 associated with variation in SW and DM using a dataset comprising 170 accessions and 74K  
194 single nucleotide polymorphisms (SNPs). We employed a comprehensive approach that  
195 integrated four GWAS analytical methods, namely the Mixed Linear Model (MLM),  
196 Compressed Mixed Linear Model (CMLM), Fixed and random model Circulating Probability  
197 Unification (FarmCPU), and Bayesian-information and Linkage-disequilibrium Iteratively  
198 Nested Keyway (BLINK). In addition, we harnessed the power of five machine learning  
199 algorithms, which included Random Forest (RF), Support Vector Regression (SVR),  
200 Convolutional Neural Networks (CNN), Artificial Neural Networks (ANN), and Support  
201 Vector Machines (SVM). This integrated approach allowed us to assess the association between  
202 SNP markers and estimated genotypic values (BLUEs) for each trait.

203

204 For MLM, CMLM, FarmCPU, and BLINK methods, we made use of the Genomic Association  
205 and Prediction Integrated Tool (GAPIT) version 2 (Lipka et al., 2012) in conjunction with the  
206 rMVP packages (Yin et al., 2021). Our association analyses were performed while correcting  
207 for both population structure and relationships among individuals, with the incorporation of  
208 either the Q+K matrices. The K matrix was computed using the Van Raden method (Lipka et  
209 al., 2012). The significance threshold for genome-wide association was determined based on a  
210 false discovery rate (FDR-adjusted  $p < 0.05$ ).

211

212 In the case of machine learning algorithms, we utilized a scaled method (ranging from 0 to 100)  
213 to estimate the importance of each SNP associated with the traits of interest. To integrate the  
214 machine learning approach into GWAS, we implemented a five-fold cross-validation strategy  
215 with ten repetitions to estimate the variable importance of each SNP, following (Siegmann and  
216 Jarmer, 2015). Therefore, we applied a global empirical threshold, as proposed by (Churchill  
217 and Doerge, 1994; Doerge and Churchill, 1996). This threshold was determined by fitting the  
218 ML algorithm, recording SNPs with the highest variable importance scores, repeating the  
219 process 1000 times, and selecting associated SNPs based on  $\alpha = 0.5$ . The machine learning  
220 methods were executed using the Caret package (Kuhn et al., 2020) in R software version 4.2.2.  
221 Throughout these analyses, we ensured that association analysis was conducted while  
222 correcting for both population structure and relationships among individuals, using a  
223 combination of the Q + K matrices. The p-value threshold for significance in the genome-wide  
224 association was determined based on a false discovery rate (FDR-adjusted  $p \leq 0.05$ ).

225

## 226 **Identification of candidate genes and haplotype analysis**

227 To identify candidate genes contributing to SW and DM, we defined haplotype blocks  
228 containing the peak SNP. Each region with the peak SNP was visually explored for its LD  
229 structure and for genes located in such regions, and the annotated genes within each interval  
230 were screened thanks to the annotated and ordered reference genome sequence in place by  
231 (International Wheat Genome Sequencing Consortium (IWGSC), 2018). Candidate genes  
232 potentially involved in each trait were further investigated. The function of these genes was  
233 also inferred by a BLAST of their sequences to the UniProt reference protein database  
234 (<http://www.uniprot.org/blast/>). To further provide more information about potential candidate  
235 genes, we used RNA-seq data of (Ramírez-González et al., 2018), based on the electronic  
236 fluorescent pictograph (eFP) at [bar.utoronto.ca/eplant](http://bar.utoronto.ca/eplant) (by (Waese et al., 2017) to identify in  
237 what tissues and at which developmental stages candidate genes were expressed in wheat.

238 To better define the possible alleles in a strong candidate gene and trait, we defined haplotypes  
239 around the peak SNP. For each haplotype, we calculated the trait mean for lines sharing the  
240 same haplotype using the R ggpubr program.

241

## 242 **Results**

### 243 **Phenotypic characterization**

244 In order to delve into the traits of SW and DM in wheat, we meticulously assessed their  
245 phenotypes over the span of two years at two distinct sites. As summarized in Table 1, the  
246 observed means ( $\pm$  standard deviation) for these traits were as follows: 5.35 ( $\pm$ 1.56) for SW and  
247 98.06 days ( $\pm$ 4.65) for DM. The broad-sense heritability estimates were robust, measuring 55.4%  
248 for SW and 50% for DM. An analysis of variance uncovered noteworthy differences attributable  
249 to genotypes (G) for all traits, and, in the case of SW and DM, the interaction between genotype  
250 and environment (GxE) also emerged as a significant factor. A correlation analysis unveiled a  
251 highly significant positive correlation between SW and DM ( $r = 0.273$ ;  $p < 0.01$ ).

252 Upon scrutinizing the relationship between SW and DM using bagplots analysis with the 170  
253 accessions in our collection, no outliers were detected when considering the interplay between  
254 these two traits (Supplementary Figure S1). Consequently, for subsequent analyses including  
255 those involving population structure and genome-wide association studies (GWAS), all  
256 accessions were retained. The distribution of phenotypic traits appeared to approximate a  
257 normal distribution and exhibited characteristics of quantitative inheritance (Figure 1).

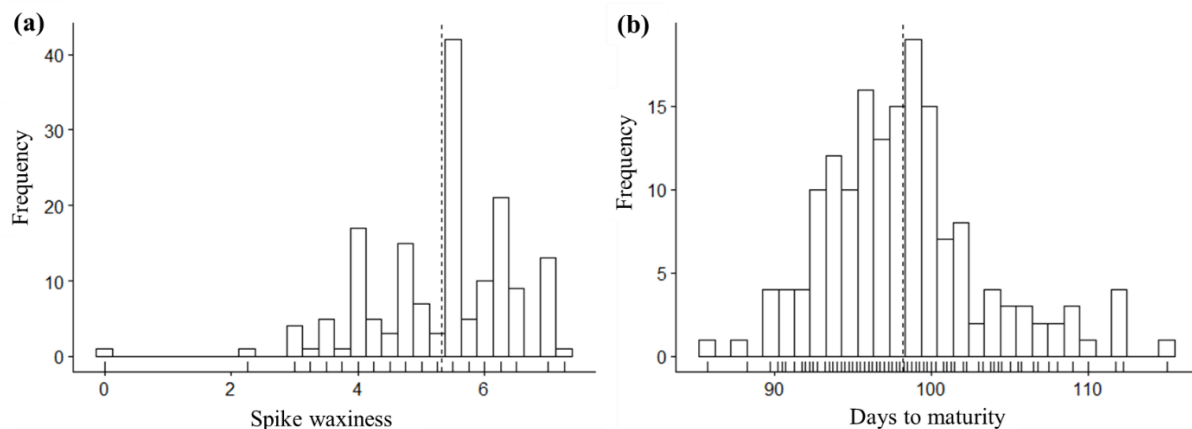
258

259 Table 1. Descriptive statistics, broad-sense heritability ( $h^2$ ), and F-values from variance  
260 analysis for two key agronomic traits in a cohort of 170 wheat lines.

| Traits | $R^2$ | CV     | Range | Mean $\pm$ SD | $h^2$            |      | F-values        |                    |        |
|--------|-------|--------|-------|---------------|------------------|------|-----------------|--------------------|--------|
|        |       |        |       |               |                  |      | Genotype<br>(G) | Environment<br>(E) | G x E  |
|        |       |        |       |               | Min              | Max  |                 |                    |        |
| SW     | 0.665 | 29.181 | 0     | 8             | 5.35 $\pm$ 1.56  | 55.4 | 1.45***         | 66.87              | 0.14   |
| DM     | 0.852 | 4.744  | 74    | 125           | 98.06 $\pm$ 4.65 | 50   | 3.39***         | 310.38**           | 3.39** |

261 SD Standard deviation,  $h^2$  Broad sense heritability,  $R^2$ : R-squared; CV: Coefficient of  
262 variation; \*\*\*, \*\* and \*: significant at  $p < 0.001$ ,  $p < 0.01$ , and  $p < 0.05$ , respectively.

263



264

265 Figure 1. Distribution of phenotypes for spike waxiness (a) and days-to-maturity (b).  
266 Histograms are based on the average trait value of each wheat line across the different  
267 environments. The bars under the histograms represent the density of individuals.

268

## 269 **Genome coverage and population structure**

270 Our comprehensive analysis revealed a total of 73,784 polymorphic SNP markers that spanned  
271 across the 21 chromosomes of the wheat genome, as depicted in Figure 2. As previously  
272 reported in our prior study, the examination of population structure within the accessions of this  
273 association panel revealed that  $K=6$  provided the optimal representation of population structure  
274 within this set of accessions. These clusters notably aligned with the geographic regions of  
275 origin. The distribution of wheat accessions among these six subpopulations ranged from 6 to  
276 43, with the largest number of accessions hailing from northwestern Baja California, Mexico,  
277 specifically represented by Mexico 1 (43). Conversely, the smallest subpopulation was  
278 observed in East and Central Africa, encompassing just 6 accessions.



279

280 Fig 2. Genome coverage of polymorphic SNP markers over the physical map of the 21  
281 chromosomes of the hexaploid wheat lines. The color reflects the density of SNP markers (i.e.  
282 number of SNPs within a sliding 1-Mb window).

283

#### 284 **Marker-trait associations**

285 To uncover the genomic regions responsible for the variation in SW and DM, we conducted an  
286 association analysis (GWAS) on a subset of accessions with phenotypic data (170 accessions  
287 and 73,784 SNPs). In this analysis, we employed four GWAS analytical tools (MLM, CMLM,  
288 FarmCPU, and BLINK), complemented by five machine learning techniques (RF, ANN, SVR,  
289 CNN, and SVM). Notably, the quantile-quantile (QQ) plots in Figure 3 demonstrated the  
290 effective control of confounding effects related to population structure and relatedness by all  
291 conventional GWAS and machine learning models. Deviations from the diagonal were  
292 observed only for the most extreme p-values, indicating a well-controlled analysis for both  
293 traits.

294

295 For the SW trait, the results of the association analyses are visualized in the Manhattan plots  
296 presented in Figure 3. Using a threshold for false discovery rate (FDR) of  $\leq 0.05$  (as detailed in  
297 Supplementary Figure S2, marked by the green horizontal line), we identified four QTLs.  
298 Remarkably, only one QTL was co-identified by at least two models (Figure 4). The most robust  
299 and consistent association, located on chromosome 1A, is summarized in Table 2.

300 This particular QTL was defined by its peak SNP, marked as chr1A:556842331, and was  
301 identified by the multi-locus models (FarmCPU and BLINK) as well as all five machine  
302 learning algorithms (RF, ANN, SVR, CNN, and SVM). Notably, this QTL explained a  
303 substantial 50% of the phenotypic variation observed in SW. The minor allele frequency (MAF)  
304 at this locus was 0.09, and it exhibited an allelic effect of 0.66.

305 These findings highlight a significant and consistent genetic association with SW on  
306 chromosome 1A, showcasing the power of both traditional GWAS and machine learning  
307 approaches in identifying key genomic regions influencing this trait.

308

309 Turning our attention to the DM trait, our investigation unveiled a total of eight genomic regions  
310 that displayed significant associations. The results of these association analyses are visualized  
311 in the Manhattan plots featured in Figure 3, with a stringent threshold for false discovery rate  
312 (FDR) of  $\leq 0.05$ , as outlined in Supplementary Figure S2 and highlighted by the green  
313 horizontal line. However, we noted the co-identification of only four Quantitative Trait Loci  
314 (QTLs) by at least two models (Figure 3). Among these, the most robust associations, localized  
315 on chromosomes 4B, 5A, and 2A, are thoughtfully summarized in Table 2.

316 Of noteworthy mention is chr4B:666048201, which emerged as the peak SNP and was jointly  
317 identified by both multi-locus GWAS models (FarmCPU and BLINK) and four machine  
318 learning algorithms (RF, ANN, SVR, and CNN). These markers formed a robust linkage block,  
319 with all markers exhibiting perfect linkage disequilibrium (LD) ( $r^2 = 1$ ), as detailed in  
320 Supplementary Table S1. This discovery delineated a single QTL, with the peak SNP  
321 accounting for a substantial 19.3% of the phenotypic variation associated with DM. The minor  
322 allele frequency (MAF) at this locus was observed to be 0.08, while the allelic effect amounted  
323 to 3.84 days (Table 2).

324 In addition, another noteworthy association with DM on chromosome 4B was unveiled, defined  
325 by the peak SNP chr4B:37907825. This association was identified by the GWAS model BLINK  
326 and all five machine learning methods (RF, ANN, SVR, CNN, and SVM). It explained 18.44%  
327 of the phenotypic variation for DM, with a MAF of 0.09 and an allelic effect of -2.76 days.

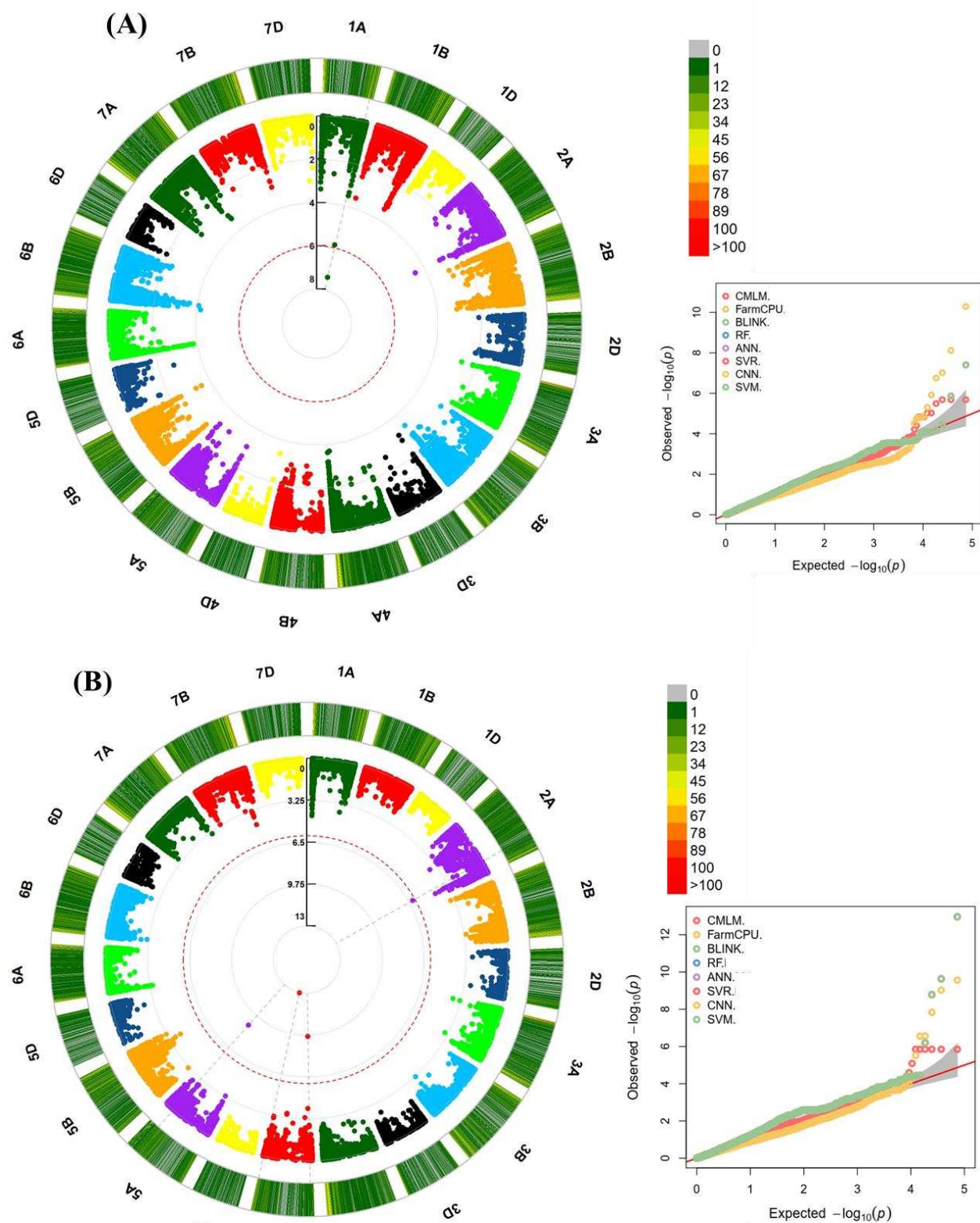
328 Moreover, a QTL residing on chromosome 2A was brought to light, marked by the peak SNP  
329 chr2A:605016602, which explained 8.65% of the phenotypic variation for DM. This QTL was  
330 detected using both multi-locus GWAS models (FarmCPU and BLINK) and all five machine  
331 learning methods (RF, ANN, SVR, CNN, and SVM).

332 Furthermore, an additional QTL on chromosome 5A, characterized by the peak SNP  
333 chr5A:580797118, was identified through the BLINK model and all five machine learning  
334 methods (RF, ANN, SVR, CNN, and SVM). This QTL contributed to 0.72% of the phenotypic  
335 variation associated with DM.

336 These findings underscore the efficacy of our approach in uncovering key genomic regions  
337 associated with DM and highlight the potential of both traditional GWAS and machine learning  
338 techniques in unraveling the genetic underpinnings of complex traits.

339  
340 Overall, the GWAS and ML methods successfully mitigated the confounding effects of population  
341 structure and relatedness and identified multiple genomic regions associated with spike waxiness  
342 and Days to maturity in wheat. These findings can provide insights into the genetic architecture of  
343 these traits and aid plant breeders in developing new bread wheat varieties with improved SW and  
344 maturity.

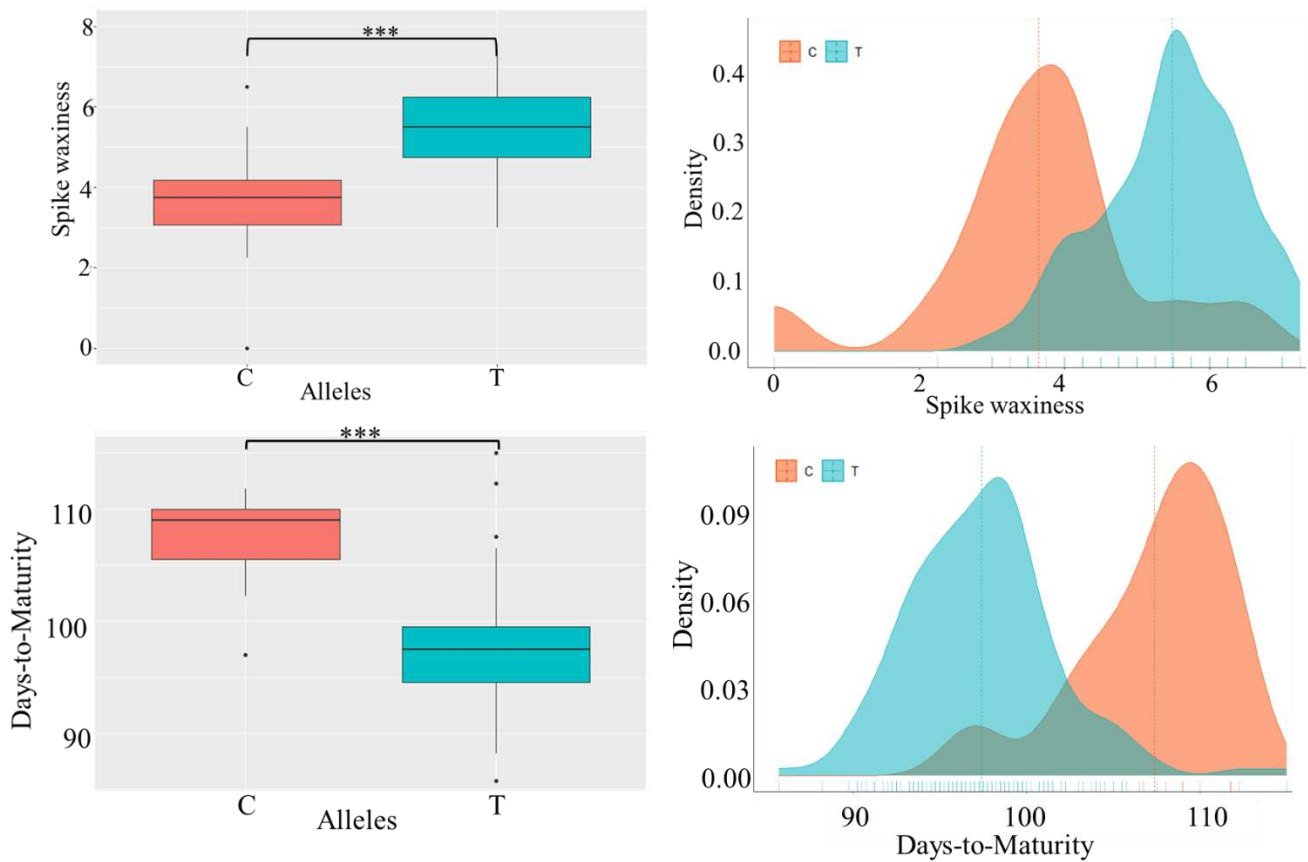
345  
346  
347  
348  
349  
350  
351  
352  
353



356 Figure 3. Genome-wide association analysis of 170 hexaploid wheat cultivars. Manhattan and  
357 Q-Q plots for all models shows the degree of association between SNPs and SW (A) and DM  
358 (B). In both cases, associations are declared significant at an FDR  $\leq 0.05$ . One marker (see the  
359 red circle) displayed significant associations with the SW trait. Four SNP markers (see the red  
360 circle) displayed significant associations with the DM.

361 In order to gain a deeper understanding of the relationship between the peak SNP  
362 (chr1A:556842331) and SW, we delved into the realm of SNP haplotypes. Through a thorough  
363 analysis of haplotypes encompassing this peak marker, we unveiled two distinct haplotypes  
364 (Figure 4). Remarkably, we observed a notable divergence in phenotypic outcomes between  
365 these haplotypes. Haplotype TT displayed significantly higher values (5.481) compared to the  
366 values associated with haplotype CC (3.642). This revelation suggests that SNP markers  
367 flanking this gene could serve as valuable tools in marker-assisted breeding programs. By  
368 selecting alleles that contribute to drought-resistant wheat varieties, these programs hold the  
369 potential to enhance wheat productivity and bolster its resilience in the face of water scarcity.  
370 To further refine our understanding of the association between the peak SNP  
371 (chr4B:666048201) and DM, we embarked on an exploration of SNP haplotypes. This  
372 investigation uncovered two distinct haplotypes encircling the peak SNP. Notably, our scrutiny  
373 of these haplotypes revealed a substantial difference in phenotypic outcomes (Figure 4).  
374 Haplotype TT was linked to significantly lower values (97.41) in comparison to haplotype CC  
375 (107.36). This observation posits that SNP markers flanking this gene have the potential to be  
376 valuable assets in marker-assisted breeding programs. By selecting alleles conducive to the  
377 development of short-season wheat varieties, these programs can contribute to the improvement  
378 of wheat productivity and the creation of cultivars better equipped to thrive in varying  
379 environmental conditions. More details are provided in Supplementary Table S2.

380



381

382 Figure 4. Boxplots (lef) and bimodal distribution (right) of Spike Waxiness and Days-to-maturity  
383 are represented for each haplotype. \*\*\*: significant at  $P < 0.001$

384 Table 2 Details of loci associated with phenotypic traits identified by at least two methods in wheat.

| Traits | Loci            | P.value  | MAF  | Allelic effect | PVE(%) | Alleles (Maj/Min) | Models                           |
|--------|-----------------|----------|------|----------------|--------|-------------------|----------------------------------|
| SW     | Chr1A:556842331 | 3.95E-08 | 0.09 | 0.66           | 50.00  | T/C               | BLINK/FarmCPU/RF/ANN/SVR/CNN/SVM |
|        | Chr4B:666048201 | 2.73E-10 | 0.08 | -3.84          | 19.3   | T/C               | FarmCPU/BLINK/RF/ANN/SVR/CNN     |
| DM     | Chr4B:37907825  | 2.32E-10 | 0.09 | -2.76          | 18.44  | T/C               | BLINK/RF/ANN/SVR/CNN/SVM         |
|        | Chr2A:605016602 | 6.36E-07 | 0.06 | 2.39           | 8.65   | G/A               | FarmCPU/BLINK/RF/ANN/SVR/CNN/SVM |
|        | Chr5A:580797118 | 1.64E-09 | 0.09 | -2.28          | 10.72  | C/T               | BLINK/RF/ANN/SVR/CNN/SVM         |

385 SW: Spike Waxiness; DM: Days to Maturity; MAF: Minor Allele Frequency; PVE: Phenotype\_Variance\_Explained (%).

386 Three conventional GWAS analytical tools, including CMLM (Compressed Mixed Linear Model); FarmCPU (Fixed and random model Circulating  
 387 Probability Unification) and BLINK (Bayesian-information and Linkage-disequilibrium Iteratively Nested Keyway), completed by five machine  
 388 learning algorithms, which included RF (Random Forest), SVR (Support Vector Regression), SNN (Convolutional Neural Networks), ANN  
 389 (Artificial Neural Networks), and SVM (Support Vector Machines) were used. The most highly associated SNP within each QTL is indicated along  
 390 with the associated statistics of RF model.

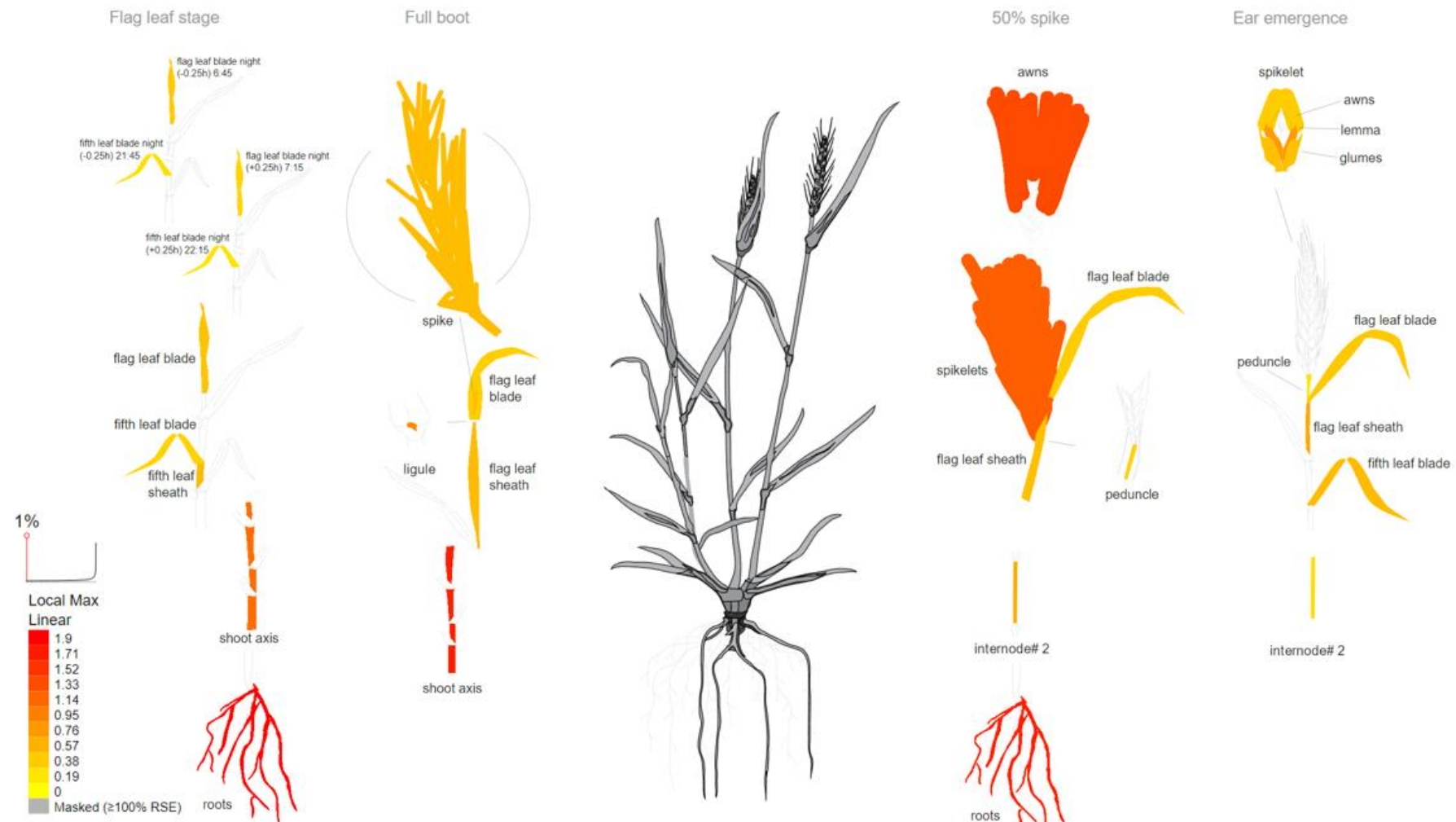
391

392 **Identification of candidate genes**

393 To pinpoint the candidate genes that potentially govern SW and DM in our diverse wheat  
394 collection, we conducted an analysis of the genes located within the same linkage block as the  
395 peak SNP for each QTL.

396 In the genomic interval encompassing the QTL that contributes the most to the phenotypic  
397 variation in SW (50%) specifically, the region from 1A\_555 to 557 Mb, surrounding the peak  
398 SNP (chr1A:556842331), we identified a total of 24 high-confidence genes. Upon a detailed  
399 examination of the gene annotations and expression profiles, one gene, TraesCS1A01G385500  
400 on chromosome 1A, emerged as the most promising candidate. TraesCS1A01G385500 is an  
401 ortholog of the *Arabidopsis Thaliana* O-acyltransferase gene, commonly known as WSD1, a  
402 bifunctional wax ester synthase/diacylglycerol acyltransferase, involved in cuticular wax  
403 biosynthesis and essential for reducing leaf water loss, particularly during drought conditions.  
404 WSD1 has also been associated with the biosynthesis of very long-chain (VLC) wax esters,  
405 contributing to drought tolerance in *Arabidopsis*. This gene exhibits the highest expression  
406 levels in spike, roots, and shoot axis tissues (Figure 5). More details are provided in  
407 Supplementary Table S3.

408 In our quest to identify potential candidate genes governing DM trait in our diverse wheat  
409 collection, we performed a meticulous analysis of the genes residing within the same linkage  
410 block as the peak SNP for each QTL. Within the genomic interval encompassing the QTL that  
411 makes the most substantial contribution to the phenotypic variation in DM (comprising 19.3%  
412 of the total variation), specifically spanning from 4B\_666 to 668 Mb and surrounding the peak  
413 SNP (chr4B:666048201), we pinpointed a total of 27 high-confidence genes. Through an in-  
414 depth examination of gene annotations and expression profiles, no one emerged as the most  
415 promising candidate. More details are provided in Supplementary Table S3.



416

417 Figure 5. Expression profile of *TraesCS1A01G385500* gene based on transcriptomic analysis in wheat. As shown, this gene is most expressed in spike,  
 418 roots and shoot axis and the image was generated with the eFP (RNA-Seq data) at <http://bar.utoronto.ca/eplant/> by Waese et al.51. The legend at  
 419 bottom left presents the expression levels, coded by colors (yellow=low, red=high).

420 **Comparison of ML and conventional GWAS methods for identifying genomic regions**

421

422 In our study, the peak SNP position on chr1A:556842331 exhibited the highest allelic effect  
423 (0.66) and explained a substantial phenotypic variance (50%) among all the identified SNPs  
424 associated with wheat SW trait. These associations were successfully detected using both  
425 GWAS models (BLINK and FarmCPU) and five machine learning algorithms (RF, ANN, SVR,  
426 CNN, and SVM). Importantly, conventional methods (MLM and CMLM) failed to identify this  
427 peak SNP linked to the SW trait (Supplementary Table S4). Furthermore, the machine learning  
428 models produced significantly lower p-values (CNN, RF, SVM, SVR, and ANN, all with p-  
429 values of 3.95E-08) compared to conventional GWAS models (CMLM with a p-value of 5.97E-  
430 05, MLM with a p-value of 5.97E-05, FarmCPU with a p-value of 6.34E-03, and BLINK with  
431 a p-value of 3.95E-08).

432 Shifting our focus to the DM trait, our investigation revealed the co-identification of four QTLs  
433 on chromosomes 4B, 5A, and 2A (with peak SNPs chr4B:666048201, chr4B:37907825,  
434 chr5A:580797118, and chr2A:605016602) by both GWAS models (BLINK and FarmCPU) and  
435 the five machine learning algorithms (RF, ANN, SVR, CNN, and SVM). The details of these  
436 robust associations are succinctly presented in Table 2. Regrettably, conventional methods  
437 (MLM and CMLM) were unable to detect these SNP peaks associated with the DM trait.  
438 Additionally, the machine learning models yielded significantly lower p-values for each of the  
439 associated markers compared to conventional GWAS models (Supplementary Table S4).

440 For the SNP chr4B:666048201, the machine learning models generated markedly lower p-  
441 values (CNN, RF, SVM, SVR, and ANN, all with p-values of 1.09E-13) compared to  
442 conventional GWAS models (CMLM with a p-value of 1.42E-06, MLM with a p-value of  
443 1.42E-06, FarmCPU with a p-value of 2.73E-10, and BLINK with a p-value of 1.09E-13).

444 For the SNP chr4B:37907825, the machine learning models produced substantially lower p-  
445 values (CNN, RF, SVM, SVR, and ANN, all with p-values of 2.32E-10) compared to  
446 conventional GWAS models (CMLM with a p-value of 2.65E-04, MLM with a p-value of  
447 2.65E-04, FarmCPU with a p-value of 4.81E-04, and BLINK with a p-value of 2.32E-10).

448 For the SNP chr5A:580797118, the machine learning models yielded notably lower p-values  
449 (CNN, RF, SVM, SVR, and ANN, all with p-values of 1.64E-09) compared to conventional  
450 GWAS models (CMLM with a p-value of 4.72E-04, MLM with a p-value of 4.72E-04, and  
451 FarmCPU with a p-value of 1, and BLINK with a p-value of 1.64E-09).

452 For the SNP chr2A:605016602, the machine learning models generated significantly lower p-  
453 values (CNN, RF, SVM, SVR, and ANN, all with p-values of 1.64E-09) compared to

454 conventional GWAS models (CMLM with a p-value of 1.38E-01, MLM with a p-value of  
455 1.38E-01, and FarmCPU with a p-value of 8.63E-02, and BLINK with a p-value of 6.36E-07).  
456

457 In essence, these traditional methods used for genetic data analysis and the establishment of  
458 associations between genetic variations and traits have limitations when it comes to identifying  
459 subtle or minor effects of certain SNPs on SW and DM characteristics in wheat. On the contrary,  
460 machine learning algorithms, particularly in conjunction with the recent multi-locus GWAS  
461 models (BLINK and FarmCPU), exhibited superior performance in identifying relevant QTLs  
462 when compared to traditional MLM and CMLM methods.

463

#### 464 **Discussion**

465 In this study, we employed four GWAS models and five machine learning algorithms to  
466 investigate the genomic regions associated with spike waxiness and days to maturity within a  
467 dataset consisting of 170 accessions and 74K SNPs. Our analyses consistently identified a  
468 robust QTL located on chromosome 1A, demonstrating significance across both conventional  
469 GWAS models (FarmCPU and BLINK) and a variety of machine learning models (BLINK,  
470 RF, ANN, SVR, CNN, and SVM). Notably, the peak SNP (chr1A:556842331) within this QTL  
471 explained a substantial portion, 50%, of the phenotypic variation observed. Within the genomic  
472 interval encompassed by this QTL (1A\_555 to 557 Mb) and centered around the peak SNP  
473 (chr1A:556842331), we identified a total of 24 high-confidence genes. Upon closer  
474 examination of gene annotations and expression profiles, one candidate gene,  
475 *TraesCS1A01G385500* on chromosome 1A, stood out as particularly promising. This gene  
476 exhibits high expression levels in spike, roots, and shoot axis tissues and shares orthology with  
477 the *Arabidopsis Thaliana* O-acyltransferase gene, widely known as the *WSD1* gene. Previous  
478 research has highlighted the significance of the *WSD1* gene, which serves as a bifunctional wax  
479 ester synthase/diacylglycerol acyltransferase (Li et al., 2008; Patwari et al., 2019). Its  
480 involvement in cuticular wax biosynthesis is well-documented, and it plays a pivotal role in  
481 reducing leaf water loss, particularly during drought conditions (Li et al., 2008; Patwari et al.,  
482 2019). The *WSD1* gene has also been associated with the biosynthesis of very long chain (VLC)  
483 wax esters, contributing to drought tolerance in *Arabidopsis* (Patwari et al., 2019). VLC primary  
484 alcohols and acyl-CoAs serve as precursors for wax ester biosynthesis, catalyzed by the  
485 bifunctional wax ester synthase/diacylglycerol acyltransferase *WSD1* (Li et al., 2008; Patwari  
486 et al., 2019). These wax components, including VLC fatty acids, aldehydes, alkanes, alcohols,  
487 ketones, and esters, undergo trafficking through the Golgi and trans-Golgi network (TGN)

488 pathways to the plasma membrane (PM). From there, they are exported to the cuticle via ABCG  
489 subfamily half transporters and lipid transfer proteins (LTPs) (DeBono et al., 2009; Ichino and  
490 Yazaki, 2022; Pighin et al., 2004; Wang and Chang, 2022).

491 Moreover, prior studies have revealed the role of AtCER1 in VLC alkane biosynthesis in  
492 Arabidopsis (Aarts et al., 1995; Bourdenx et al., 2011; Sakuradani et al., 2013). Recently, He  
493 et al. (2022) identified a homologous gene of AtCER1 in wheat, named TaCER1-6A, which  
494 shares 55% amino acid identity with AtCER1. Similar to previously reported AtCER1  
495 orthologs, including rice OsCER1 (Ni et al., 2018), wheat TaCER1-1A (Li et al., 2019),  
496 Brachypodium BdCER1-8 (Wu et al., 2019), cucumber CsCER1 (W. Wang et al., 2015), and  
497 *P. pratensis* PpCER1 (Wang et al., 2021), TaCER1-6A also contains three specific His-rich  
498 motifs essential for VLC alkane biosynthesis (Bernard et al., 2012). Therefore, (He et al., 2022)  
499 speculated that TaCER1-6A likely plays a similar role in VLC alkane biosynthesis in wheat.  
500 Notably, we observed that alleles associated with higher wax content were more prevalent in  
501 lines originating from East African spring-type accessions (Kenya and Ethiopia) and North  
502 Africa. These accessions primarily consist of spring lines cultivated in arid regions and were  
503 acquired from the International Center for Agricultural Research in the Dry Areas (ICARDA).  
504 Ultimately, our study has unveiled a promising candidate gene, *TraesCS1A01G385500*, linked  
505 to spike waxiness, with implications for cuticular wax biosynthesis and its role in drought  
506 tolerance, as established in previous research. This discovery sheds light on the genetic  
507 mechanisms underpinning spike waxiness in bread wheat, offering valuable insights for future  
508 breeding and crop improvement efforts.

509 Regarding DM, we identified four strong genomic regions significantly associated with the trait  
510 on chromosomes 4B, 2A and 5A. Our results were consistent with those of (Semagn et al.,  
511 2021), who performed QTL mapping in four RIL populations evaluated under conventional and  
512 organic management systems and reported two QTLs associated with days to maturity on  
513 chromosome 4B (explaining 20.8% of the phenotypic variances), where one (QMat.dms-4B.2)  
514 at chr4B:569184188-599613837 is located on the extremity of long chromosome 4B arm with  
515 the peak SNP chr4B:666048201 (explaining 19.3% of the phenotypic variation) that was jointly  
516 identified by both multi-locus GWAS models and four ML algorithms (RF, ANN, SVR, and  
517 CNN) in the present study. QTL mapping conducted by previous authors (Zou et al., 2017a,  
518 2017b) in the ‘Attila’ and ‘CDC Go’ RIL populations using genetic maps of 1203 markers  
519 identified a coincident genomic region associated with maturity under both management  
520 systems on chromosome 4B and 5A. We also identified QTLs on chromosomes 4B and 5A,

521 with peak SNPs chr4B:666048201, chr4B:37907825, and chr5A:580797118 explaining 19.3%,  
522 18.44%, and 10.72%, of the phenotypic variation, respectively. The favorable alleles for those  
523 QTLs on 4B and 5A were most originated from the accessions of North Africa, including spring  
524 lines (Attila) acquired from the International Center for Agricultural Research in the Dry Areas  
525 (ICARDA). Interesting, previous works also identified two QTLs for maturity on chromosome  
526 4B (QMat.dms-4B) and chromosome 5A (QMat.dms-5A.2), which individually explained  
527 15.9% and 14.0% of the phenotypic variance, respectively, and together accounted for 29.9%  
528 of the phenotypic variance across seven environments (Zou et al., 2017a, 2017b). The favorable  
529 alleles for QMat.dms-4B and QMat.dms-5A.2 originated from 'Attila' and 'CDC Go',  
530 respectively. (Chen et al., 2020) also identified a QTL associated with maturity on chromosome  
531 4B (4B\_s4991673- 4B\_d1258252) using a linkage map of 4439 markers produced by DArTseq  
532 technology and phenotype data from 'Peace' and 'Carberry' RIL populations assessed for two  
533 years under organic management and conventional systems, consistent with our results.  
534 Our investigation into candidate genes associated with maturity in wheat led us to a genomic  
535 interval spanning the QTL that contributes significantly to the phenotypic variation in Days-to-  
536 Maturity (19.3% of the variation). This region, located between 4B\_666 and 668 Mb and  
537 centered around the peak SNP (chr4B:666048201), contained a total of 27 high-confidence  
538 genes. Our findings align with prior research that has identified genomic regions on  
539 chromosome 4B associated with maturity and housing candidate genes related to flower-  
540 promoting factors. Notably, certain dwarfing genes, such as Rht-B1, Rht5, Rht8, and Rht12,  
541 have been reported to exert slight delays in heading, flowering, and/or maturity time in wheat.  
542 These genetic factors add complexity to the regulation of these traits (Chen et al., 2018; Daoura  
543 Goudia et al., 2014). The discovery in the present study contributes to our understanding of the  
544 genetic factors underpinning wheat maturity and sets the stage for future research aimed at  
545 elucidating the molecular mechanisms involved.  
546 The results our study highlight the remarkable superiority of machine learning (ML) models in  
547 identifying significant genetic associations compared to traditional Genome-Wide Association  
548 Study (GWAS) methods, as demonstrated through substantially lower p-values. For SW, the  
549 peak SNP was efficiently identified by both GWAS models (BLINK and FarmCPU) and the  
550 five ML algorithms, emphasizing their robustness. Notably, the ML models, including CNN,  
551 RF, SVM, SVR, and ANN, produced significantly lower p-values (3.95E-08) compared to the  
552 traditional GWAS models, which had p-values ranging from 5.97E-05 to 6.34E-03. Traditional  
553 methods (MLM and CMLM) failed to detect this critical SNP, showcasing their limitations in  
554 capturing minor genetic effects. Shifting the focus to DM, the robust associations identified by

555 GWAS models and ML algorithms demonstrated that conventional methods (MLM and  
556 CMLM) were less effective, failing to detect these essential SNP peaks. Once again, ML models  
557 consistently delivered significantly lower p-values, underscoring their increased sensitivity and  
558 accuracy in identifying genetic markers linked to DM. The differences in p-values were  
559 substantial, with ML models consistently outperforming the traditional GWAS methods.  
560 These findings reveal that traditional GWAS methods face limitations in detecting minor  
561 genetic effects on SW and DM traits in wheat. Conversely, ML models, especially when  
562 coupled with advanced multi-locus GWAS models like BLINK and FarmCPU, exhibited a  
563 superior performance characterized by significantly lower p-values. This work demonstrates  
564 the potential of ML approaches to revolutionize the study of complex genetic traits, offering  
565 valuable insights for crop improvement and stress resilience in bread wheat. Our hypotheses  
566 (1) regarding the presence of specific genomic regions associated with SW and DM in a diverse  
567 global collection of bread wheat accessions and (2) the superior performance of Machine  
568 Learning-Genome-Wide Association Study (ML-GWAS) approaches over traditional GWAS  
569 methods in identifying relevant genomic regions associated with SW and DM traits in bread  
570 wheat have been confirmed. Our study has provided evidence that conventional GWAS  
571 approaches, such as MLM, and CMLM, lack the ability to effectively detect SNPs with minor  
572 effects underlying specific traits. In other words, these traditional methods used to analyze  
573 genetic data and establish associations between genetic variations and traits are not sensitive  
574 enough to identify subtle or minor effects of certain SNPs on the characteristics of SW and DM  
575 in wheat. These findings align with previous research conducted by (Yoosefzadeh-Najafabadi  
576 et al., 2023; Zhou et al., 2019), which also highlighted the limited power of conventional GWAS  
577 approaches in detecting SNPs with minor effects on specific traits.  
578 However, our study has revealed the effectiveness of an alternative approach, utilizing machine  
579 learning algorithms in GWAS. By employing this method, we were able to overcome the  
580 limitations of traditional GWAS and more accurately identify SNPs with smaller yet significant  
581 effects on SW and DM traits in wheat. Additionally, the most robust associations identified by  
582 modern GWAS methodologies (BLINK and FarmCPU) were reaffirmed by machine learning  
583 techniques. These results are consistent with the studies conducted by (Yoosefzadeh-Najafabadi  
584 et al., 2023) and (Zhou et al., 2019), which compared SVR and RF algorithms, respectively, to  
585 conventional GWAS methods in soybean. They reported that machine learning algorithms are  
586 more accurate and sensitive in detecting subtle or minor effects of certain SNPs on traits of  
587 interest. Additionally, our study demonstrated the effectiveness of the new GWAS model,  
588 BLINK and FarmCPU, in accurately and efficiently detecting SNPs with smaller but significant

589 effects on SW and DM traits in wheat. In fact, both real and simulated data analyses have shown  
590 that BLINK significantly improves statistical power compared to FarmCPU, while also  
591 reducing computing time (Huang et al., 2019).

592 The FarmCPU, developed by (Liu et al., 2016), represents an iterative method that addresses  
593 the issue of false positive control and confounding between testing markers and cofactors  
594 simultaneously. As FarmCPU tests markers in a fixed-effect model, it is computationally more  
595 efficient than methods that test markers in a random-effect model, such as MLM, CMLM,  
596 ECMLM, SUPER, and MLMM (Liu et al., 2016). Studies have demonstrated the order of the  
597 statistical power of these methods: BLINK > FarmCPU > CMLM > MLM (Huang et al., 2019;  
598 Liu et al., 2016; Zhang et al., 2010).

599 The utilization of machine learning algorithms (RF, ANN, SVR, CNN, and SVM), along with  
600 the recent multi-locus GWAS model, BLINK, and FarmCPU has enabled a more sensitive and  
601 precise identification of genetic factors influencing specific traits. This opens up new  
602 opportunities for wheat improvement and selection. Indeed, ML algorithms are focused on  
603 maximizing prediction accuracy at the individual subject level and have been shown to capture  
604 multi-locus SNP interactions better than univariate association studies (Okser et al., 2014,  
605 2013). Additionally, ML techniques provide an opportunity to better understand multi-locus  
606 genetic variants and their interactions in predicting complex traits (Ashkenazy et al., 2022;  
607 Kwon et al., 2022). This approach provides a more sophisticated and reliable means of  
608 discovering genetic markers associated with SW and DM traits, which can have significant  
609 implications for agriculture, varietal selection, and understanding the genetic mechanisms  
610 governing crop characteristics.

611 Overall, both GWAS and machine learning methods have successfully addressed the  
612 confounding effects of population structure and relatedness, allowing us to identify multiple  
613 genomic regions associated with SW and DM traits in wheat. These findings shed light on the  
614 genetic architecture of these traits and offer valuable insights to plant breeders in their efforts  
615 to develop new bread wheat varieties with improved SW and DM.

616

617

618

619

620

621

622 **Conclusion**

623 In this study, our primary objective was to identify the genomic regions associated with SW  
624 and DM using state-of-the-art Machine Learning-Genome-Wide Association Study (ML-  
625 GWAS) techniques. Our findings provide a deep understanding of the genetic landscape  
626 governing these critical traits, delivering valuable insights that can significantly inform wheat  
627 breeding and crop improvement strategies. Leveraging ML-GWAS, we successfully identified  
628 a robust QTL significantly associated with SW on chromosome 1A, represented by the peak  
629 SNPs chr1A:556842331, explaining an impressive 50% of the phenotypic variation.  
630 Additionally, we detected four strong genomic regions significantly associated with DM on  
631 chromosomes 4B, 2A, and 5A, employing the same cutting-edge methods. Notably, our study  
632 unveiled a candidate gene linked to the QTLs for SW. *TraesCS1A01G385500*, an ortholog of  
633 the *Arabidopsis Thaliana* O-acyltransferase gene *WSD1*, plays a pivotal role in cuticular wax  
634 biosynthesis. It is essential for reducing leaf water loss, particularly during drought conditions,  
635 and contributes to drought tolerance through the biosynthesis of very long-chain (VLC) wax  
636 esters. Our study also shows that, ML models, especially when coupled with advanced multi-  
637 locus GWAS models like BLINK and FarmCPU, exhibited a superior performance  
638 characterized by significantly lower p-values in identifying relevant QTLs compared to  
639 traditional methods like MLM and CMLM. This work demonstrates the potential of ML  
640 approaches to revolutionize the study of complex genetic traits, offering valuable insights for  
641 crop improvement and stress resilience in bread wheat. ML-GWAS emerges as a compelling  
642 approach for genomic-based breeding strategies, providing breeders with more accurate and  
643 efficient tools to develop improved wheat varieties. Our research significantly advances the  
644 precision and effectiveness of GWAS, emphasizing the importance of incorporating advanced  
645 computational methods into crop breeding studies. The insights into the genetic architecture of  
646 SW and DM traits in wheat offer essential knowledge for designing targeted crop improvement  
647 strategies. Moreover, the versatility and effectiveness demonstrated by the ML-GWAS  
648 approach extend its applicability beyond wheat and can be harnessed to address other crop  
649 traits, thus enhancing progress in crop genetics research and breeding efforts on a broader scale.  
650 Overall, the integration of machine learning techniques with GWAS stands as a potent tool for  
651 dissecting complex traits in crop genetics research. The findings of our study hold great promise  
652 for the field of wheat breeding and crop improvement strategies, making substantial  
653 contributions to enhancing agricultural productivity and ensuring food security in the face of  
654 evolving global challenges.

655 **Additional Information** Supplementary information for this paper is available at:

656 **Competing interests:** The authors declare that they have no competing interests.

657 **Acknowledgements:**

658 Authors are grateful to the International Maize and Wheat Improvement Center (CIMMYT),  
659 the International Center for Agricultural Research in the Dry Areas (ICARDA) and the Plant  
660 Breeding Laboratory (Department of Genetics, Stellenbosch University) for their technical  
661 supports and wheat varieties collection. We would like to thank Dr Wuletaw Tadesse, Mr Tsimi  
662 Patrick, Mr Charly Mam for their technical support. We are grateful to Dr Amina Abed and Dr  
663 Jérôme Laroche for their technical support during bioinformatics analyses.

664

665 **References**

666 Aarts, M.G., Keijzer, C.J., Stiekema, W.J., Pereira, A., 1995. Molecular characterization of  
667 the CER1 gene of *arabidopsis* involved in epicuticular wax biosynthesis and pollen  
668 fertility. *Plant Cell* 7, 2115–2127. <https://doi.org/10.1105/tpc.7.12.2115>

669 Ashkenazy, N., Feder, M., Shir, O.M., Hübner, S., 2022. GWANN: Implementing deep  
670 learning in genome wide association studies.  
671 <https://doi.org/10.1101/2022.06.01.494275>

672 Belzile, F., Abed, A., Torkamaneh, D., 2020. Time for a paradigm shift in the use of plant  
673 genetic resources. *Genome* 63, 189–194. <https://doi.org/10.1139/gen-2019-0141>

674 Bernard, A., Domergue, F., Pascal, S., Jetter, R., Renne, C., Faure, J.-D., Haslam, R.P.,  
675 Napier, J.A., Lessire, R., Joubès, J., 2012. Reconstitution of plant alkane biosynthesis  
676 in yeast demonstrates that *Arabidopsis ECERIFERUM1* and *ECERIFERUM3* are core  
677 components of a very-long-chain alkane synthesis complex. *Plant Cell* 24, 3106–3118.  
678 <https://doi.org/10.1105/tpc.112.099796>

679 Bourdenx, B., Bernard, A., Domergue, F., Pascal, S., Léger, A., Roby, D., Pervent, M., Vile,  
680 D., Haslam, R.P., Napier, J.A., Lessire, R., Joubès, J., 2011. Overexpression of  
681 *Arabidopsis ECERIFERUM1* promotes wax very-long-chain alkane biosynthesis and  
682 influences plant response to biotic and abiotic stresses. *Plant Physiol.* 156, 29–45.  
683 <https://doi.org/10.1104/pp.111.172320>

684 Chen, H., Bemister, D.H., Iqbal, M., Strelkov, S.E., Spaner, D.M., 2020. Mapping genomic  
685 regions controlling agronomic traits in spring wheat under conventional and organic  
686 managements. *Crop Sci.* 60, 2038–2052. <https://doi.org/10.1002/csc2.20157>

687 Chen, L., Du, Y., Lu, Q., Chen, H., Meng, R., Cui, C., Lu, S., Yang, Y., Chai, Y., Li, J., Liu,  
688 L., Qi, X., Li, H., Mishina, K., Yu, F., Hu, Y.-G., 2018. The Photoperiod-Insensitive  
689 Allele *Ppd-D1a* Promotes Earlier Flowering in *Rht12* Dwarf Plants of Bread Wheat.  
690 *Front. Plant Sci.* 9.

691 Churchill, G.A., Doerge, R.W., 1994. Empirical threshold values for quantitative trait  
692 mapping. *Genetics* 138, 963–971. <https://doi.org/10.1093/genetics/138.3.963>

693 Daoura Goudia, B., Chen, L., Yingying, D., Yingang, H., 2014. Genetic effects of dwarfing  
694 gene *Rht-5* on agronomic traits in common wheat (*Triticum aestivum* L.) and QTL  
695 analysis on its linked traits. *Field Crops Res.* 156, 22–29.  
696 <https://doi.org/10.1016/j.fcr.2013.10.007>

697 DeBono, A., Yeats, T.H., Rose, J.K.C., Bird, D., Jetter, R., Kunst, L., Samuels, L., 2009.  
698 *Arabidopsis LTPG Is a Glycosylphosphatidylinositol-Anchored Lipid Transfer Protein*  
699 *Required for Export of Lipids to the Plant Surface.* *Plant Cell* 21, 1230–1238.  
700 <https://doi.org/10.1105/tpc.108.064451>

701 Doerge, R.W., Churchill, G.A., 1996. Permutation Tests for Multiple Loci Affecting a  
702 Quantitative Character. *Genetics* 142, 285–294.  
703 <https://doi.org/10.1093/genetics/142.1.285>

704 Doyle, J.J., Doyle, J.L., 1990. Isolation of plant DNA from fresh tissue. *Focus* 12, 39–40.  
705 Elshire, R.J., Glaubitz, J.C., Sun, Q., Poland, J.A., Kawamoto, K., Buckler, E.S., Mitchell,  
706 S.E., 2011. A Robust, Simple Genotyping-by-Sequencing (GBS) Approach for High  
707 Diversity Species. *PLoS ONE* 6, e19379.  
708 <https://doi.org/10.1371/journal.pone.0019379>

709 Enoma, D.O., Bishung, J., Abiodun, T., Ogunlana, O., Osamor, V.C., 2022. Machine learning  
710 approaches to genome-wide association studies. *J. King Saud Univ. - Sci.* 34, 101847.  
711 <https://doi.org/10.1016/j.jksus.2022.101847>

712 He, J., Li, C., Hu, N., Zhu, Y., He, Z., Sun, Y., Wang, Z., Wang, Y., 2022. ECERIFERUM1-  
713 6A is required for the synthesis of cuticular wax alkanes and promotes drought  
714 tolerance in wheat. *Plant Physiol.* 190, 1640–1657.  
715 <https://doi.org/10.1093/plphys/kiac394>

716 Hen-Avivi, S., Savin, O., Racovita, R.C., Lee, W.-S., Adamski, N.M., Malitsky, S.,  
717 Almekias-Siegl, E., Levy, M., Vautrin, S., Bergès, H., Friedlander, G., Kartvelishvily,  
718 E., Ben-Zvi, G., Alkan, N., Uauy, C., Kanyuka, K., Jetter, R., Distelfeld, A., Aharoni,  
719 A., 2016. A Metabolic Gene Cluster in the Wheat W1 and the Barley Cer-cqu Loci  
720 Determines  $\beta$ -Diketone Biosynthesis and Glaucousness. *Plant Cell* 28, 1440–1460.  
721 <https://doi.org/10.1105/tpc.16.00197>

722 Huang, M., Liu, X., Zhou, Y., Summers, R.M., Zhang, Z., 2019. BLINK: a package for the  
723 next level of genome-wide association studies with both individuals and markers in  
724 the millions. *GigaScience* 8, giy154. <https://doi.org/10.1093/gigascience/giy154>

725 Ichino, T., Yazaki, K., 2022. Modes of secretion of plant lipophilic metabolites via ABCG  
726 transporter-dependent transport and vesicle-mediated trafficking. *Curr. Opin. Plant  
727 Biol.* 66, 102184. <https://doi.org/10.1016/j.pbi.2022.102184>

728 Ingram, G., Nawrath, C., 2017. The roles of the cuticle in plant development: organ adhesions  
729 and beyond. *J. Exp. Bot.* 68, 5307–5321. <https://doi.org/10.1093/jxb/erx313>

730 International Wheat Genome Sequencing Consortium (IWGSC), 2018. Shifting the limits in  
731 wheat research and breeding using a fully annotated reference genome. *Science* 361,  
732 eaar7191. <https://doi.org/10.1126/science.aar7191>

733 Iqbal, M., Navabi, A., Salmon, D.F., Yang, R.-C., Murdoch, B.M., Moore, S.S., Spaner, D.,  
734 2007. Genetic analysis of flowering and maturity time in high latitude spring wheat.  
735 *Euphytica* 154, 207–218. <https://doi.org/10.1007/s10681-006-9289-y>

736 Kaler, A.S., Gillman, J.D., Beissinger, T., Purcell, L.C., 2020. Comparing Different Statistical  
737 Models and Multiple Testing Corrections for Association Mapping in Soybean and  
738 Maize. *Front. Plant Sci.* 10, 1794. <https://doi.org/10.3389/fpls.2019.01794>

739 Kamran, A., Iqbal, M., Navabi, A., Randhawa, H., Pozniak, C., Spaner, D., 2013. Earliness  
740 per se QTLs and their interaction with the photoperiod insensitive allele Ppd-D1a in  
741 the Cutler  $\times$  AC Barrie spring wheat population. *Theor. Appl. Genet.* 126, 1965–1976.  
742 <https://doi.org/10.1007/s00122-013-2110-0>

743 Kamran, Atif, Randhawa, H.S., Pozniak, C., Spaner, D., 2013. Phenotypic Effects of the  
744 Flowering Gene Complex in Canadian Spring Wheat Germplasm. *Crop Sci.* 53, 84–  
745 94. <https://doi.org/10.2135/cropsci2012.05.0313>

746 Kosma, D.K., Bourdenx, B., Bernard, A., Parsons, E.P., Lü, S., Joubès, J., Jenks, M.A., 2009.  
747 The impact of water deficiency on leaf cuticle lipids of *Arabidopsis*. *Plant Physiol.*  
748 151, 1918–1929. <https://doi.org/10.1104/pp.109.141911>

749 Kuhn, M., Wing, J., Weston, S., Williams, A., Keefer, C., Engelhardt, A., Cooper, T., Mayer,  
750 Z., Kenkel, B., Team, R.C., 2020. Package ‘*caret*.’ *R J.* 223.

751 Kunst, L., Samuels, L., 2009. Plant cuticles shine: advances in wax biosynthesis and export.  
752 *Curr. Opin. Plant Biol.* 12, 721–727. <https://doi.org/10.1016/j.pbi.2009.09.009>

753 Kwon, O.-S., Hong, M., Kim, T.-H., Hwang, I., Shim, J., Choi, E.-K., Lim, H.E., Yu, H.T.,  
754 Uhm, J.-S., Joung, B., Oh, S., Lee, M.-H., Kim, Y.-H., Pak, H.-N., 2022. Genome-  
755 wide association study-based prediction of atrial fibrillation using artificial  
756 intelligence. *Open Heart* 9, e001898. <https://doi.org/10.1136/openhrt-2021-001898>

757 Li, F., Wu, X., Lam, P., Bird, D., Zheng, H., Samuels, L., Jetter, R., Kunst, L., 2008.  
758 Identification of the Wax Ester Synthase/Acyl-Coenzyme A:Diacylglycerol  
759 Acyltransferase WSD1 Required for Stem Wax Ester Biosynthesis in *Arabidopsis*.  
760 *Plant Physiol.* 148, 97–107. <https://doi.org/10.1104/pp.108.123471>

761 Li, T., Sun, Y., Liu, T., Wu, H., An, P., Shui, Z., Wang, J., Zhu, Y., Li, C., Wang, Y., Jetter,  
762 R., Wang, Z., 2019. TaCER1-1A is involved in cuticular wax alkane biosynthesis in  
763 hexaploid wheat and responds to plant abiotic stresses. *Plant Cell Environ.* 42, 3077–  
764 3091. <https://doi.org/10.1111/pce.13614>

765 Lipka, A.E., Tian, F., Wang, Q., Peiffer, J., Li, M., Bradbury, P.J., Gore, M.A., Buckler, E.S.,  
766 Zhang, Z., 2012. GAPIT: genome association and prediction integrated tool.  
767 *Bioinforma. Oxf. Engl.* 28, 2397–2399. <https://doi.org/10.1093/bioinformatics/bts444>

768 Liu, X., Huang, M., Fan, B., Buckler, E.S., Zhang, Z., 2016. Iterative Usage of Fixed and  
769 Random Effect Models for Powerful and Efficient Genome-Wide Association Studies.  
770 *PLOS Genet.* 12, e1005767. <https://doi.org/10.1371/journal.pgen.1005767>

771 Martin, L.B.B., Rose, J.K.C., 2014. There’s more than one way to skin a fruit: formation and  
772 functions of fruit cuticles. *J. Exp. Bot.* 65, 4639–4651.  
773 <https://doi.org/10.1093/jxb/eru301>

774 Mohammadi, M., Xavier, A., Beckett, T., Beyer, S., Chen, L., Chikssa, H., Cross, V., Freitas  
775 Moreira, F., French, E., Gaire, R., Griebel, S., Lopez, M.A., Prather, S., Russell, B.,  
776 Wang, W., 2020. Identification, deployment, and transferability of quantitative trait  
777 loci from genome-wide association studies in plants. *Curr. Plant Biol.* 24, 100145.  
778 <https://doi.org/10.1016/j.cpb.2020.100145>

779 Ni, E., Zhou, L., Li, J., Jiang, D., Wang, Z., Zheng, S., Qi, H., Zhou, Y., Wang, C., Xiao, S.,  
780 Liu, Z., Zhou, H., Zhuang, C., 2018. OsCER1 Plays a Pivotal Role in Very-Long-  
781 Chain Alkane Biosynthesis and Affects Plastid Development and Programmed Cell  
782 Death of Tapetum in Rice (*Oryza sativa* L.). *Front. Plant Sci.* 9, 1217.  
783 <https://doi.org/10.3389/fpls.2018.01217>

784 Nicholls, H.L., John, C.R., Watson, D.S., Munroe, P.B., Barnes, M.R., Cabrera, C.P., 2020.  
785 Reaching the End-Game for GWAS: Machine Learning Approaches for the  
786 Prioritization of Complex Disease Loci. *Front. Genet.* 11.

787 Okser, S., Pahikkala, T., Airola, A., Salakoski, T., Ripatti, S., Aittokallio, T., 2014.  
788 Regularized Machine Learning in the Genetic Prediction of Complex Traits. *PLOS*  
789 *Genet.* 10, e1004754. <https://doi.org/10.1371/journal.pgen.1004754>

790 Okser, S., Pahikkala, T., Aittokallio, T., 2013. Genetic variants and their interactions in  
791 disease risk prediction - machine learning and network perspectives. *BioData Min.* 6,  
792 5. <https://doi.org/10.1186/1756-0381-6-5>

793 Pask, A.J.D., Pietragalla, J., Mullan, D.M., Reynolds, M.P., 2012. Physiological breeding II: a  
794 field guide to wheat phenotyping. *Cimmyt.*

795 Patwari, P., Salewski, V., Gutbrod, K., Kreszies, T., Dresen-Scholz, B., Peisker, H., Steiner,  
796 U., Meyer, A.J., Schreiber, L., Dörmann, P., 2019. Surface wax esters contribute to  
797 drought tolerance in *Arabidopsis*. *Plant J. Cell Mol. Biol.* 98, 727–744.  
798 <https://doi.org/10.1111/tpj.14269>

799 Pighin, J.A., Zheng, H., Balakshin, L.J., Goodman, I.P., Western, T.L., Jetter, R., Kunst, L.,  
800 Samuels, A.L., 2004. Plant cuticular lipid export requires an ABC transporter. *Science*  
801 306, 702–704. <https://doi.org/10.1126/science.1102331>

802 Ramírez-González, R.H., Borrill, P., Lang, D., Harrington, S.A., Brinton, J., Venturini, L.,  
803 Davey, M., Jacobs, J., van Ex, F., Pasha, A., Khedikar, Y., Robinson, S.J., Cory, A.T.,  
804 Florio, T., Concia, L., Juery, C., Schoonbeek, H., Steuernagel, B., Xiang, D., Ridout,  
805 C.J., Chalhoub, B., Mayer, K.F.X., Benhamed, M., Latrasse, D., Bendahmane, A.,  
806 International Wheat Genome Sequencing Consortium, Wulff, B.B.H., Appels, R.,  
807 Tiwari, V., Datla, R., Choulet, F., Pozniak, C.J., Provart, N.J., Sharpe, A.G., Paux, E.,  
808 Spannagl, M., Bräutigam, A., Uauy, C., 2018. The transcriptional landscape of  
809 polyploid wheat. *Science* 361, eaar6089. <https://doi.org/10.1126/science.aar6089>

810 Sakuradani, E., Zhao, L., Haslam, T.M., Kunst, L., 2013. The CER22 gene required for the  
811 synthesis of cuticular wax alkanes in *Arabidopsis thaliana* is allelic to CER1. *Planta*  
812 237, 731–738. <https://doi.org/10.1007/s00425-012-1791-y>

813 Semagn, K., Iqbal, M., Chen, H., Perez-Lara, E., Bemister, D.H., Xiang, R., Zou, J., Asif, M.,  
814 Kamran, A., N'Diaye, A., Randhawa, H., Pozniak, C., Spaner, D., 2021. Physical  
815 Mapping of QTL in Four Spring Wheat Populations under Conventional and Organic  
816 Management Systems. I. Earliness. *Plants* 10, 853.  
817 <https://doi.org/10.3390/plants10050853>

818 Seo, P.J., Lee, S.B., Suh, M.C., Park, M.-J., Go, Y.S., Park, C.-M., 2011. The MYB96  
819 transcription factor regulates cuticular wax biosynthesis under drought conditions in  
820 *Arabidopsis*. *Plant Cell* 23, 1138–1152. <https://doi.org/10.1105/tpc.111.083485>

821 Siegmann, B., Jarmer, T., 2015. Comparison of different regression models and validation  
822 techniques for the assessment of wheat leaf area index from hyperspectral data. *Int. J.  
823 Remote Sens.* 36, 4519–4534. <https://doi.org/10.1080/01431161.2015.1084438>

824 Snape, J., Butterworth, K., Whitechurch, E., Worland, A.J., 2001. Waiting for Fine Times:  
825 Genetics of Flowering Time in Wheat, in: Bedö, Z., Láng, L. (Eds.), *Wheat in a  
826 Global Environment: Proceedings of the 6th International Wheat Conference*, 5–9  
827 June 2000, Budapest, Hungary, *Developments in Plant Breeding*. Springer  
828 Netherlands, Dordrecht, pp. 67–74. [https://doi.org/10.1007/978-94-017-3674-9\\_7](https://doi.org/10.1007/978-94-017-3674-9_7)

829 Tekeu, H., Ngonkeu, E.L.M., Bélanger, S., Djocgoué, P.F., Abed, A., Torkamaneh, D., Boyle,  
830 B., Tsimi, P.M., Tadesse, W., Jean, M., Belzile, F., 2021. GWAS identifies an  
831 ortholog of the rice D11 gene as a candidate gene for grain size in an international  
832 collection of hexaploid wheat. *Sci. Rep.* 11, 19483. <https://doi.org/10.1038/s41598-021-98626-0>

833 Tekeu, H., Ngonkeu, E.M.L., Djocgoué, F.P., Ellis, A., Lendzemo, V., Springfield, L.,  
834 Moulin, L., Klonowska, A., Diouf, D., Botes, W.C., Bena, G., 2017. Genetic diversity  
835 of Cameroonian bread wheat (*Triticum aestivum* L.) cultivars revealed by  
836 microsatellite markers. *Afr. J. Biotechnol.* 16, 1832–1839.  
837 <https://doi.org/10.5897/AJB2017.16090>

838 Torkamaneh, D., Laroche, J., Bastien, M., Abed, A., Belzile, F., 2017. Fast-GBS: a new  
839 pipeline for the efficient and highly accurate calling of SNPs from genotyping-by-  
840 sequencing data. *BMC Bioinformatics* 18, 1–7.

841 Waese, J., Fan, J., Pasha, A., Yu, H., Fucile, G., Shi, R., Cumming, M., Kelley, L.A.,  
842 Sternberg, M.J., Krishnakumar, V., Ferlanti, E., Miller, J., Town, C., Stuerzlinger, W.,  
843 Provart, N.J., 2017. ePlant: Visualizing and Exploring Multiple Levels of Data for

844

845 Hypothesis Generation in Plant Biology. *Plant Cell* 29, 1806–1821.  
 846 <https://doi.org/10.1105/tpc.17.00073>

847 Wang, D., Ni, Y., Liao, L., Xiao, Y., Guo, Y., 2021. *Poa pratensis* ECERIFERUM1  
 848 (PpCER1) is involved in wax alkane biosynthesis and plant drought tolerance. *Plant*  
 849 *Physiol. Biochem. PPB* 159, 312–321. <https://doi.org/10.1016/j.plaphy.2020.12.032>

850 Wang, W., Zhang, Y., Xu, C., Ren, J., Liu, X., Black, K., Gai, X., Wang, Q., Ren, H., 2015.  
 851 Cucumber ECERIFERUM1 (CsCER1), which influences the cuticle properties and  
 852 drought tolerance of cucumber, plays a key role in VLC alkanes biosynthesis. *Plant*  
 853 *Mol. Biol.* 87, 219–233. <https://doi.org/10.1007/s11103-014-0271-0>

854 Wang, X., Chang, C., 2022. Exploring and exploiting cuticle biosynthesis for abiotic and  
 855 biotic stress tolerance in wheat and barley. *Front. Plant Sci.* 13, 1064390.  
 856 <https://doi.org/10.3389/fpls.2022.1064390>

857 Wang, Y., Wang, M., Sun, Y., Hegebarth, D., Li, T., Jetter, R., Wang, Z., 2015a. Molecular  
 858 Characterization of TaFAR1 Involved in Primary Alcohol Biosynthesis of Cuticular  
 859 Wax in Hexaploid Wheat. *Plant Cell Physiol.* 56, 1944–1961.  
 860 <https://doi.org/10.1093/pcp/pcv112>

861 Wang, Y., Wang, M., Sun, Y., Wang, Yanting, Li, T., Chai, G., Jiang, W., Shan, L., Li, C.,  
 862 Xiao, E., Wang, Z., 2015b. FAR5, a fatty acyl-coenzyme A reductase, is involved in  
 863 primary alcohol biosynthesis of the leaf blade cuticular wax in wheat (*Triticum*  
 864 *aestivum* L.). *J. Exp. Bot.* 66, 1165–1178. <https://doi.org/10.1093/jxb/eru457>

865 Wu, H., Shi, S., Lu, X., Li, T., Wang, J., Liu, T., Zhang, Q., Sun, W., Li, C., Wang, Z., Chen,  
 866 Y., Quan, L., 2019. Expression Analysis and Functional Characterization of CER1  
 867 Family Genes Involved in Very-Long-Chain Alkanes Biosynthesis in *Brachypodium*  
 868 *distachyon*. *Front. Plant Sci.* 10, 1389. <https://doi.org/10.3389/fpls.2019.01389>

869 Yin, L., Zhang, H., Tang, Z., Xu, J., Yin, D., Zhang, Z., Yuan, X., Zhu, M., Zhao, S., Li, X.,  
 870 Liu, X., 2021. rMVP: A Memory-efficient, Visualization-enhanced, and Parallel-  
 871 accelerated Tool for Genome-wide Association Study. *Genomics Proteomics*  
 872 *Bioinformatics* 19, 619–628. <https://doi.org/10.1016/j.gpb.2020.10.007>

873 Yousefzadeh Najafabadi, M., Tulpan, D., Eskandari, M., 2021. Using Hybrid Artificial  
 874 Intelligence and Evolutionary Optimization Algorithms for Estimating Soybean Yield  
 875 and Fresh Biomass Using Hyperspectral Vegetation Indices. *Remote Sens.* 13, 2555.  
 876 <https://doi.org/10.3390/rs13132555>

877 Yousefzadeh-Najafabadi, M., Torabi, S., Tulpan, D., Rajcan, I., Eskandari, M., 2023.  
 878 Application of SVR-Mediated GWAS for Identification of Durable Genetic Regions  
 879 Associated with Soybean Seed Quality Traits. *Plants* 12, 2659.  
 880 <https://doi.org/10.3390/plants12142659>

881 Yu, J., Buckler, E.S., 2006. Genetic association mapping and genome organization of maize.  
 882 *Curr. Opin. Biotechnol.* 17, 155–160. <https://doi.org/10.1016/j.copbio.2006.02.003>

883 Zadoks, J.C., Chang, T.T., Konzak, C.F., 1974. A decimal code for the growth stages of  
 884 cereals. *Weed Res.* 14, 415–421. <https://doi.org/10.1111/j.1365-3180.1974.tb01084.x>

885 Zhang, Z., Ersoz, E., Lai, C.-Q., Todhunter, R.J., Tiwari, H.K., Gore, M.A., Bradbury, P.J.,  
 886 Yu, J., Arnett, D.K., Ordovas, J.M., Buckler, E.S., 2010. Mixed linear model approach  
 887 adapted for genome-wide association studies. *Nat. Genet.* 42, 355–360.  
 888 <https://doi.org/10.1038/ng.546>

889 Zhou, W., Bellis, E.S., Stubblefield, J., Causey, J., Qualls, J., Walker, K., Huang, X., 2019.  
 890 Minor QTLs mining through the combination of GWAS and machine learning feature  
 891 selection. <https://doi.org/10.1101/712190>

892 Zou, J., Semagn, K., Iqbal, M., Chen, H., Asif, M., N'Diaye, A., Navabi, A., Perez-Lara, E.,  
 893 Pozniak, C., Yang, R.-C., Randhawa, H., Spaner, D., 2017a. QTLs associated with  
 894 agronomic traits in the Attila × CDC Go spring wheat population evaluated under

895 conventional management. PLOS ONE 12, e0171528.  
896 <https://doi.org/10.1371/journal.pone.0171528>  
897 Zou, J., Semagn, K., Iqbal, M., N'Diaye, A., Chen, H., Asif, M., Navabi, A., Perez-Lara, E.,  
898 Pozniak, C., Yang, R., Randhawa, H., Spaner, D., 2017b. Mapping QTLs Controlling  
899 Agronomic Traits in the 'Attila' × 'CDC Go' Spring Wheat Population under Organic  
900 Management using 90K SNP Arra. Crop Sci. 57, 365–377.  
901 <https://doi.org/10.2135/cropsci2016.06.0459>

902

903